Engineering Fracture Mechanics 96 (2012) 676–686

Contents lists available at SciVerse ScienceDirect

Engineering Fracture Mechanics

journal homepage: www.elsevier.com/locate/engfracmech

Mixed mode delamination growth of multidirectional composite laminates under fatigue loading

Lei Peng [a], Jifeng Xu [a,*], Jianyu Zhang [b], Libin Zhao [c]

[a] Beijing Aeronautical Science & Technology Research Institute, Beijing 102211, China
[b] Institute of Solid Mechanics, Beihang University, Beijing 100191, China
[c] School of Astronautics, Beihang University, Beijing 100191, China

ARTICLE INFO

Article history:
Received 18 April 2012
Received in revised form 10 August 2012
Accepted 21 September 2012

Keywords:
Composites
R-curves
Delamination
Fatigue crack growth

ABSTRACT

Fatigue delamination growth of multidirectional laminates with 45°/−45° fracture interface was experimentally studied. Delamination tests under three mixed I/II mode ratios were carried out via mixed mode bending test apparatus. Significant *R*-curve effects on the fatigue crack growth rates and thresholds due to fiber bridging and crack branching were observed, which make the traditional Paris Law unsuitable. In this paper, a formerly developed modified Paris Law with the normalized strain energy release rate as the fracture governing parameter is investigated again. The results from the multidirectional delamination tests fit the modified Paris Law very well, and hence have validated it by experiments. Moreover, the thresholds normalized to delamination resistance were utilized to evaluate the critical fatigue crack growth conditions. By the combination of test data for both 0°/5° and 90°/90° laminates, an interface-independent normalized threshold was proposed, which was found linearly decreasing with mode mixture ratios.

1. Introduction

Carbon fiber reinforced polymer composites are commonly used in primary aerospace structures due to the advantages such as high strength/stiffness-to-weight ratio and satisfactory durability. However, the mechanical properties of laminates are much lower in interlaminar direction than in-plane directions due to the ply-by-ply formulation of composites. Delamination therefore gains significant attention during design and analysis of composites, especially for low velocity impact, central holes and "*T*" or "π" integral joint cases.

Linear elastic fracture mechanics is widely utilized to study the interlaminar fracture of composites. Strain energy release rate (SERR) is commonly accepted as the fracture governing parameter to evaluate interlaminar fracture toughness for composites rather than the stress intensity factor (SIF) for metals. Experimental studies and test methods for delamination resistance have been reviewed by Davies et al. [1] and Brunner et al. [2].

As multidirectional laminates are generally preferred to unidirectional ones in engineering structures, an amount of studies on delamination along multidirectional interfaces have been reported in literature [3–6]. As a summarized result, multidirectional laminates always exhibit higher interlaminar fracture toughness, which is assumed to be caused by extrinsic toughening mechanisms such as blunted crack tips or deviation of the crack from the main crack plane to the adjacent layers and some in-ply energy absorption [7]. Besides, different stacking sequence, fiber orientations and crack propagation

* Corresponding author.
E-mail addresses: penglei@comac.cc (L. Peng), xujifeng@comac.cc (J. Xu), jyzhang@buaa.edu.cn (J. Zhang), lbzhao@buaa.edu.cn (L. Zhao).

0013-7944/$ - see front matter © 2012 Elsevier Ltd. All rights reserved.
http://dx.doi.org/10.1016/j.engfracmech.2012.09.033

Nomenclature

A, C'	coefficients in fatigue crack growth laws
a, a_1	delamination length
a_0	initial delamination length
b	width of test specimen
C	compliance of specimen, d/P
$\overline{C}$	normalized compliance, Cbh^3
c	lever length of MMB apparatus
c_g	lever length of MMB apparatus to center of gravity
d	displacement
E_f	axial flexural modulus
G	total strain energy release rate (SERR)
G_0	fracture toughness at the initial crack length
G_I	opening (mode I) component of SERR
G_{II}	shear (mode II) component of SERR
G_c	static delamination resistance (fracture toughness)
G_{cf}	fatigue delamination resistance
G_{max}	maximum value of cyclic SERR
G_{th}	threshold value of SERR for fatigue crack growth
g_{max}	maximum value of cyclic SERR normalized to G_{cf}
g_{th}	threshold value of SERR normalized to G_{cf}
h	half thickness of test specimen
k	slope of R-curves
L	half-span length of the MMB test apparatus
m	slope of load displacement curve
N	number of elapsed fatigue cycles
P	applied load
P_g	weight of lever and attached apparatus
p, r	exponents in fatigue crack growth laws
ΔG	SERR range during a fatigue cycle
ϵ	difference of compliance between static and fatigue specimens
ϵ_0	tolerance of compliance difference considering experimental errors
φ	mode mixture ratio, G_{II}/G
χ	crack length correction factor

directions have significant effects on the fracture mechanics and then on the interlaminar toughness of composite laminates [3], which makes multidirectional delamination studied more complex and being still open for researchers.

Another key factor which may bring considerable delamination resistance is fiber bridging, which could be enhanced by multidirectional ply orientations for certain materials. Based on bridging zone models, several fiber bridging laws have been developed [8–10] to describe the relationship of the bridging stresses and the value of crack opening displacement (COD).

For fatigue delamination propagation studies on composites, some significant fundamental works have been performed by Hojo et al. [11,12], Asp et al. [13,14], Brunner et al. [15] and other researchers[16–18]. Based on the analogy with the Paris Law for metals, early researchers have identified a linear log–log relationship between the fatigue delamination growth rate and the SERR. For multidirectional laminates and/or fiber bridging cases, however, the previously mentioned additional fracture resistance will cause the R-curve effect, which makes the conventional Paris Law unsuitable [19]. Similarly, the fatigue thresholds, below which no fatigue delamination growth occurs, were found no longer a life constant for multidirectional laminates and composites with fiber bridging. Remarkable R-curve effects on the fatigue delamination have been observed and analyzed by Hojo et al. [12] for Zanchor-reinforced laminates, Argülles et al. [20] for unidirectional laminates with fiber bridging and Shivakumar et al. [21] for woven/braided fiber composites.

To quantitatively evaluate the effect of R-curves on the fatigue crack growth, a novel concept and a "re-loading" determination method of fatigue delamination resistance, denoted by G_{cf}, has been introduced by Peng et al. [19]. A modified Paris Law taking normalized SERR as the controlling parameter was then proposed for mode I loading. Zhang et al. [22] subsequently extended the application of the normalized Paris Law to mixed I/II loading for unidirectional laminates. An advanced "compliance approach" to determine G_{cf} was also developed.

The study presented here is a continuation of that work. The capability of the normalized Paris Law on multidirectional laminates with 45°/−45° interface under mixed mode loading was examined via experiments. Effects of mode mixture ratio on the fatigue crack growth rates were studied for both unidirectional and multidirectional laminates, by assessing the fatigue constants of the normalized Paris Law. Based on the normalized threshold model, an interface-independent relationship between the fatigue thresholds and the mode I/II mixture ratio was obtained.

2. Experiment

2.1. Manufacture of specimens

The laminates with 45°/−45° ply interface were manufactured from unidirectional prepreg with a 25 μm Teflon™ insert sited at the mid-plane. The stacking sequence of specimen was $(+45/-45/0_6)_S//(-45/+45/0_6)_S$, which was carefully selected to ensure that the bend-twist coupling and antielastic effects were reduced to the minimum. The effect of 25 μm insert on mode I fracture toughness during crack initiation was studied by Peng et al. [19], and slight enhancement for 45°/−45° specimen was observed.

The material used here was T700/QY811 carbon/bismaleimide composites, the elastic properties of which are as follow: E_{11} = 130 GPa, $E_{22} = E_{33}$ = 10.4 GPa, $G_{12} = G_{13}$ = 6.36 GPa, $\nu_{12} = \nu_{13}$ = 0.3. Laminates were autoclaved according to the supplier's recommended procedures and quality assessed using ultrasonic C-scanning prior to cutting into specimens. The specimen geometric configuration is 180 mm long by 25 mm wide with a 35 mm insert. The nominal thickness of specimen is $2h$ = 4.16 mm. To visualize crack growth, the edges of specimens were painted white using a typewriter correction fluid. Unless stated otherwise, four specimens were tested for each fatigue condition.

As denoted by Hiley [23], it was important to know the position of 0° ply with respect to upper and lower fracture surfaces of the specimen in performing delamination tests, particularly when a component of shear load was applied. Due to bending of the specimen, microcracks developing ahead of the crack tip tend to propagate towards the upper (compressive) side of the laminates, unless 0° plies was set to suppress crack branching. In this study, two plies of ±45° were layered adjacent to the fracture surface, and thus intra-ply crack propagation in the upper 45° ply should be noticed during the tests.

2.2. Mode I testing

Both the static and fatigue tests in mode I were performed using the double cantilever (DCB) specimen in an MTS servo-hydraulic test machine with a 1000 N load cell. A modified version of the quick-mounted hinge design proposed by Brandt [24] was used to ensure the load was effectively applied to the middle plane of the cantilever beams. The illustration of DCB configuration is shown in Fig. 1a. A loading rate of 0.5 mm/min was used in static tests. In the fatigue tests, constant displacement amplitude testing of the specimens was performed at a frequency of 5 Hz using an R-ratio of 0.1.

Crack propagation was monitored by an instrumented traveling microscope, which is equipped with an electronic dial gage to record the position of crack tip with a precision resolution of 0.01 mm.

2.3. Mixed mode testing

Mixed I/II mode tests were conducted using the mixed mode bending (MMB) test originally proposed by Reeder and Crews [25,26]. The test procedure followed ASTM standard D6671M-06 [27], except that the quick-mounted hinges designed by Brandt [24] was used to load force on the ends of delaminated section of specimens instead of bonded hinges, as shown in Fig. 1b. Tests under three mixed mode ratios, such as 0.25, 0.50, and 0.75, were performed by adjusting lever length of the MMB apparatus.

In the static tests, a low loading rate of 0.1 mm/min was used to obtain the fracture toughness near equilibrium configuration. According to the study by Sorensen et al. [8], a high loading rate may induce significant larger fracture toughnesses than equilibrium condition, especially for fiber bridging cases. During the tests, therefore, the applied displacement was held for 10 min at certain intervals. When the hold was implemented, the crack usually continued to progress for a few millimeters until it reached a constant equilibrium position. A single lower G_c value was then measured.

In the fatigue tests, the frequency was 5 Hz and R-ratio 0.1. As it is impossible to apply infinite loading cycles to achieve the saturated thresholds, the determination of fatigue threshold values requires definition of an acceptable limit [15]. Here,

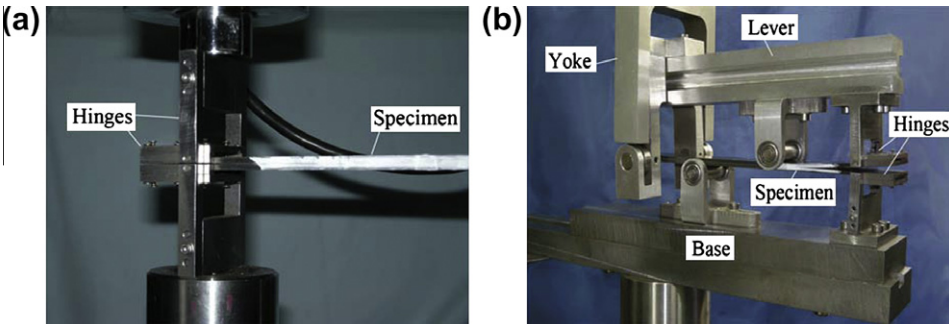

Fig. 1. Illustration of testing configuration: (a) DCB and (b) MMB.

the fatigue thresholds were determined for cases that the crack growth rate went blow 1×10^{-7} mm/cycle or no crack growth occurred for 5×10^5–1×10^6 cycles.

3. Data analysis

3.1. Analysis of SERR

For DCB tests, the SERR was calculated using the equation below [28]:

$$G_{\mathrm{I}} = \frac{3Pd}{2b(a+\chi h)} \frac{F}{N'} \tag{1}$$

where F is a correction factor for large displacements and N' a correction for load-block effect, which is equal to 1 due to the quick-mounted hinge used in this study. Also, χ a correction for crack tip displacement and rotation, which allows for the beam not being perfectly built in. Illustration of parameters P, d and a is shown in Fig. 2.

The χh value can be calculated theoretically [29] or experimentally [30] by plotting the cubic root of compliance $C^{1/3}$ as a function of crack length a and determining the intercept on the x-axis. However, great attention should be paid for fiber bridging cases where the specimen's compliance may be reduced by the bridging stresses. A wrong larger value of χ may thus be obtained by conventional data reduction method. To solve this problem, a modified approach which conducts the fitting procedure excluding experimental data within the significant fiber bridging zone was proposed by Peng et al. [19]. The calculation of χ here followed such a procedure, as significant fiber bridging was observed during tests.

The pure mode SERR for MMB test has been derived by Reeder and Crews [25]. The weight loading of the lever was accounted for and the SERR was calculated by following equation [27]:

$$G_{\mathrm{I}} = \frac{12[P(3c-L)+P_{\mathrm{g}}(3c_{\mathrm{g}}-L)]^2}{16E_{\mathrm{f}}b^2h^3L^2}(a+\chi h)^2 \tag{2}$$

$$G_{\mathrm{II}} = \frac{9[P(c+L)+P_{\mathrm{g}}(c_{\mathrm{g}}+L)]^2}{16E_{\mathrm{f}}b^2h^3L^2}(a+0.42\chi h)^2 \tag{3}$$

where P_{g} is the weight of lever and attached loading apparatus, c_{g} the lever length to center of gravity and E_{f} the bending modulus. For a given mode mixture ratio φ, the value of c could be calculated by combining Eqs. (2) and (3), which guided the setting of lever length during tests. Illustration of the parameters in the two equations could be found in Fig. 3.

3.2. Fatigue delamination modeling

The well-known Paris Law is the most commonly used method to model fatigue crack growth [13]. A simple form of Paris Law has developed by Wikins [31] and Singh and Greenhalgh [16], shown as

$$\frac{\mathrm{d}a}{\mathrm{d}N} = A(\Delta G)^p \tag{4}$$

where $\mathrm{d}a/\mathrm{d}N$ is the propagation rate of delamination, ΔG is the total SERR range, A and p are constants.

However, for multidirectional specimens the fiber bridging and/or crack branching may cause additional delamination resistance. Significant R-curve effect will make the traditional Paris Law not suitable any more. A normalized SERR, $g_{\max}$, instead of $G_{\max}$ was therefore proposed to evaluate the fatigue delamination growth rates [19], expressed as

$$g_{\max}(a) = \frac{G_{\max}(a)}{G_{\mathrm{cf}}(a)} \tag{5}$$

where $G_{\mathrm{cf}}(a)$ is the fatigue delamination growth resistance, defined as the critical energy release rate during fatigue crack growth. The modified Paris Law was thus reformed as

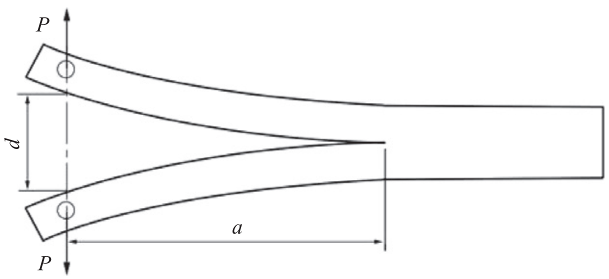

Fig. 2. Illustration of parameters in tested DCB specimen.

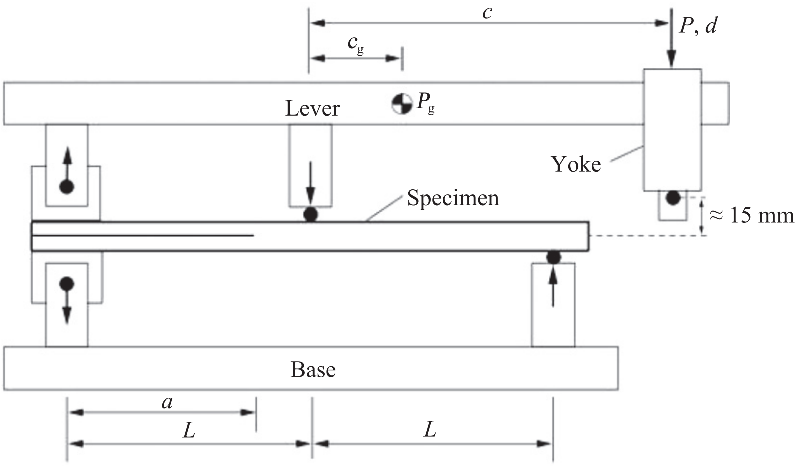

Fig. 3. Illustration of parameters in tested MMB specimen.

$$\left(\frac{da}{dN}\right)_a = C'(g_{max}(a))^r \tag{6}$$

where C' and r are new fatigue constants.

A normalized fatigue threshold parameter could also been proposed based on the fatigue delamination resistance, shown as

$$g_{th} = \frac{G_{th}}{G_{cf}} \tag{7}$$

It could be found that the most important advancement of the normalized fatigue crack growth model is the introduction of the fatigue delamination resistance, G_{cf}. As a general crack tip governing parameter, the normalized SERR take into account the effect of both driving force and resistance on fatigue crack growth.

3.3. Calculation of fatigue delamination resistance

To obtain the fatigue resistance, G_{cf}, two methods were developed by evaluating the difference between the fatigue delamination resistance and the static value, namely "re-loading approach" [19] and "compliance approach" [22] respectively. Although the two methods are theoretically equivalent, "compliance approach" is selected here due to the advantage that it does not interrupt fatigue tests and is little affected by the specimens' dimensions variation.

The approach is developed for fiber bridging cases and based on the following hypothesis: the delamination resistance of fatigue specimen is equal to the value of corresponding static specimen which exhibits the same force–displacement behavior. According to "compliance approach", the fatigue delamination resistance at certain crack length, a_1, could be determined by comparing the normalized compliance of fatigue and static specimens. The procedure was summarized and rewritten as in the following equation:

$$\begin{aligned}
&\text{if } \frac{\overline{C}_f(a_1)}{\overline{C}_s(a_1)} - 1 < -\epsilon_0 \\
&\quad G_{cf}(a_1) = G_c(a|_{\overline{C}_s(a)=\overline{C}_f(a_1)}) \\
&\text{else} \\
&\quad G_{cf}(a_1) = G_c(a_1)
\end{aligned} \tag{8}$$

where $\overline{C}$ is the normalized compliance of specimen, calculated by Eq. (9). ϵ_0 is the critical tolerance to consider experimental errors of the compliance. The subscripts "f" and "s" indicate the fatigue and static specimens, respectively.

$$\overline{C} = \frac{1}{m} bh^3 \tag{9}$$

where m is the slope of force–displacement curve of a specimen.

For delamination along multidirectional interfaces, both fiber bridging and crack branching may be the reason causing R-curve behavior [32]. To obtain fatigue delamination resistance by "compliance approach", therefore, the fracture patterns at crack tip of fatigue and static specimens should be similar, in which case the energy consumed by crack branching could be reasonably assumed equal.

4. Results and discussion

4.1. Interlaminar fracture toughness

By the visual observation from side view during tests and the fracture surface examination after final failure, significant bridging of +45° and −45° fibers was found across fracture plane. Therefore, the modified data reduction approach formerly developed for fiber bridging cases [19] was utilized and the value of crack length correction factor (χ) was obtained to be 1.67.

The fracture toughness could subsequently be determined via Eqs. (1)–(3). The typical plots of G_c versus crack length a are shown in Fig. 4 for all the four mode I/II mixture ratios. The obtained R-curves show that both the initiation and propagation values of fracture toughness increase with increasing mode mixture ratio, despite that the curves for $\varphi = 0.25$ and $\varphi = 0.50$ are really close.

Linear fit, results of which are included in Fig. 4, was found to agree well with testing data under all the conditions for the crack length between 35 mm and 55 mm. The following linear formula was therefore simply used to fit the delamination resistance,

$$G_c = G_0 + k(a - a_0) \tag{10}$$

where G_0 is the initial fracture toughness and k the slope of delamination resistance curve. Summery of a_0, G_0 and k values are given in Table 1.

For MMB tests, when the applied displacement was held at certain intervals, the crack indeed continued growing for a distance and the force decreased. The equilibrium fracture toughnesses, however, are almost the same as quasi-static conditions, less than 3% lower. It indicates that the loading speed of 0.1 mm/min slightly enlarges the measured value of fracture toughness. Hence the little differences are ignored here and the quasi-static results are adopted. For DCB tests, the above displacement holding process was not applied. It should be noted that the difference between mode I toughness and equilibrium value may be larger than mixed mode cases due to a higher loading speed of 0.5 mm/min applied.

4.2. Fatigue delamination resistance

As discussed in Section 3.3, crack branching and intra-ply crack always occur during delamination along multidirectional interfaces, which bring additional fracture resistance besides fiber bridging. It's necessary to examine the fracture pattern similarity of the fatigue and static specimens before applying the "compliance approach" to calculate the fatigue delamination resistance.

Fig. 5 shows the delamination paths of the static and fatigue specimens obtained by the instrumented traveling microscope. It could be found that crack grew almost along the middle +45°/−45° interface under pure opening loading. Shear fracture cracks within the adjacent up +45° ply occurred when mode II loads were introduced. The delamination paths are similar for both fatigue and static specimens, which implies approximate fracture patterns.

Based on the above assumption, the "compliance approach" was used to calculate the fatigue delamination resistance. The result were given in Table 2 according to Eq. (8). To study the effect of the fracture interfaces, results from 0°/5° and 90°/90° specimens were included in the table. The layups of 0°/5° and 90°/90° specimens are $0_{16}//(+5/-5/0_6)_S$ and $(90/0/90/0_5)_S//(90/0/90/0_5)_S$, respectively. Details of the laminates and tests could be found in [19,22]. The tolerance was reasonably set to be 5% consider experimental measurement errors. Thus only when the compliance from fatigue specimens are less than that from static specimens (at the same crack length) and the difference is greater than 5%, the delamination resistances are considered to be significantly different.

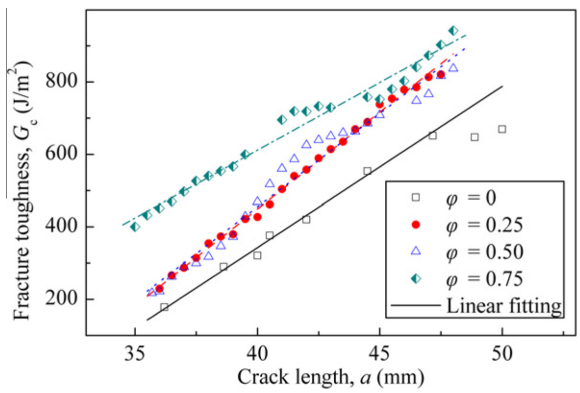

Fig. 4. Static delamination resistance versus crack length for 45°/−45° interface.

Table 1
Summary of a_0, G_0 and k values.

Mode mixture ratio, φ	a_0 (mm)	G_0 (J/m^2)	k ((J/m^2)/mm)
0.00	36.2	173.8	44.5
0.25	36.0	235.3	53.5
0.50	35.7	233.0	51.6
0.75	35.0	424.5	37.4

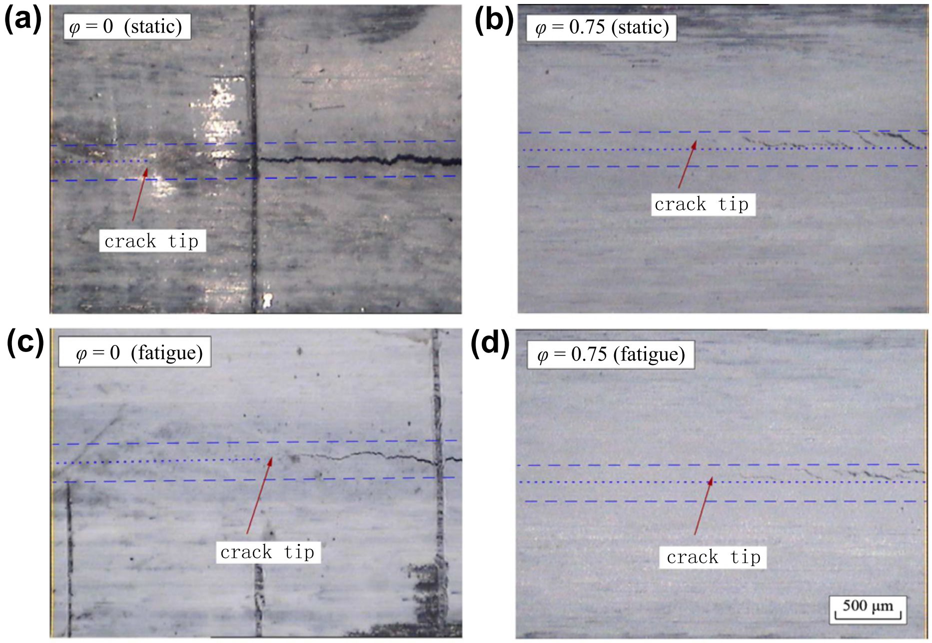

Fig. 5. Delamination growth paths from side view. (Dot lines indicate the position of the middle +45°/−45° interfaces, while dash lines indicate adjacent ply interfaces.)

Table 2
Compliance comparison between fatigue and static specimens to determine the fatigue delamination resistance. *Note:* The bold values indicate the case that satisfy the condition in Eq. (8).

Interface	Mode mixed ratio, φ	Crack Length, a (mm)	Normalized compliance, $\overline{C}$ (mm^5/N)		Difference, ϵ (%)
			Static specimen	Fatigue specimen	
45°/−45°	0.00	43.70	12.80	13.03	1.8
	0.25	42.30	16.62	17.23	3.7
	0.50	41.60	4.73	4.96	5.0
	0.75	40.88	2.59	2.69	3.5
0°/5° [22]	0.00	42.01	6.99	6.96	−0.4
	0.25	46.78	10.53	10.93	3.8
	0.50	46.60	3.34	3.36	0.7
	0.75	**47.41**	**2.16**	**1.95**	**−9.7**
90°/90° [19]	0.00	41.60	10.26	10.09	−1.6

From Table 2, the above condition is satisfied only for 0°/5° specimen under 0.75 mixture ratio. Consequently, the fatigue and static delamination resistances are most likely to be different for unidirectional specimen applied high shear force. For +45°/−45° specimens studied here, the condition in Eq. (8) was not satisfied and thus the fatigue delamination resistance was simply calculated to be equal to statically measured fracture toughness.

4.3. Fatigue delamination growth rates

The plots of the fatigue crack growth rates evaluated by the traditional and the modified Paris Law (the normalized model) were shown in Figs. 6 and 7, respectively. In the two figures, the same type of symbol under each testing condition

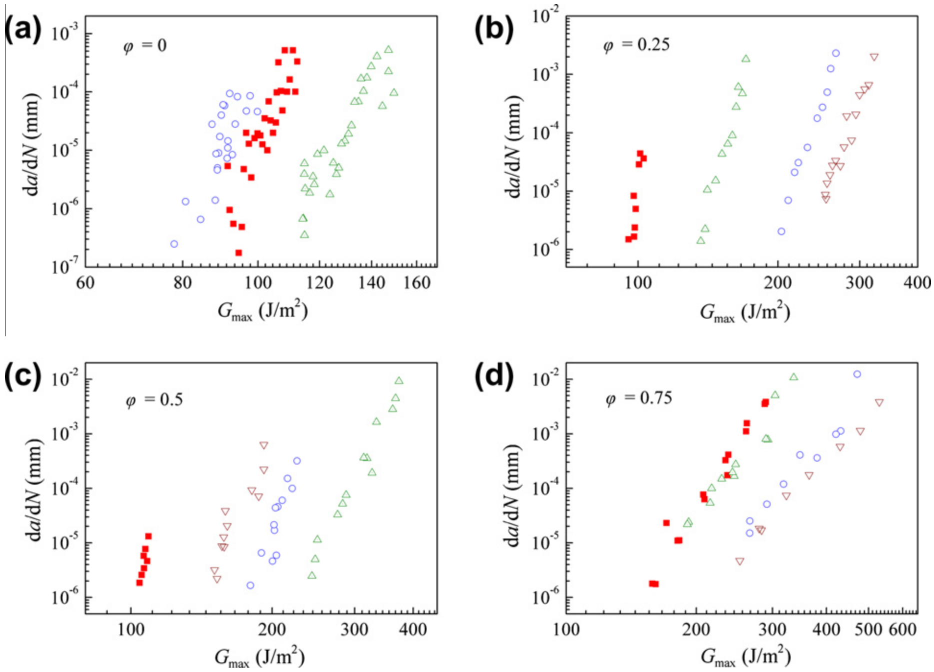

Fig. 6. Fatigue crack growth rates versus maximum SERR.

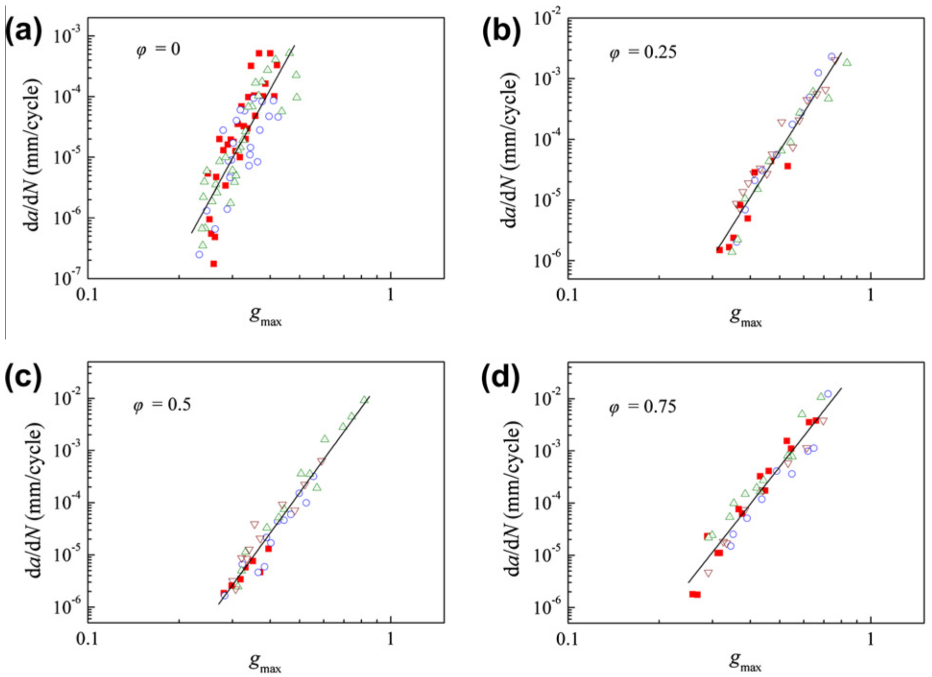

Fig. 7. Fatigue crack growth rates versus normalized SERR.

indicates experimental data measured from the same one specimen. Different specimens were applied different maximum cyclic displacements to cover a wide range of ΔG.

Obviously, the *R*-curve effect significantly changed the fatigue crack growth behavior of the laminates. The rising delamination resistance makes the traditional Paris Law no longer suitable to describe the fatigue crack growth rates. Instead, the normalized Paris Law showed excellent agreement with experimental data, validating the normalized fatigue crack growth model. Values of coefficients and exponents in the normalized Paris Law were listed in Table 3.

Table 3
Values of coefficient and exponent in normalized Paris Law.

Mode mixture ratio, φ	Coefficient, C' (mm/cycle)	Exponent, r
0.00	5.5×10^{-1}	9.1
0.25	1.6×10^{-2}	7.9
0.50	4.0×10^{-2}	8.0
0.75	8.3×10^{-2}	7.4

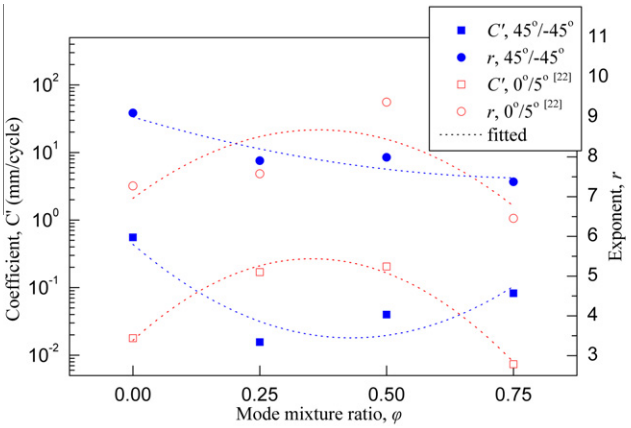

Fig. 8. Plots of life constants in the normalized Paris Law versus mode mixture ratio.

A non-monotonic polynomial model proposed by Blanco et al. [13] was used to fit the relationship between the modified Paris Law constants and mixture ratio. Results from 45°/−45° and 0°/5° specimens were presented in Fig. 8. Excellent agreement was achieved except for exponent values from 0°/5° specimens. It is obvious that the life constant curves significantly differ from each other for varied interfaces. It therefore brings great difficult to predict fatigue crack growth for multidirectional laminates, since the delamination plane and directions always varies during crack growth. As some earlier studies [14,16,33] revealed, for composites, determination of thresholds for fatigue delamination growth therefore become to be important.

4.4. Fatigue thresholds

Threshold values of SERR for delamination growth in fatigue were presented in Fig. 9. It was found that the G_{th} values increased along with the crack length and delamination resistance, which indicated that G_{th} was no longer a uniform parameter for the evaluation of fatigue thresholds.

On the contrary, the normalized thresholds, g_{th}, which take into account of the effect of delamination resistance, kept highly consistency under each test condition, as shown in Fig. 10. The normalized thresholds from 0°/5° and 90°/90° interface

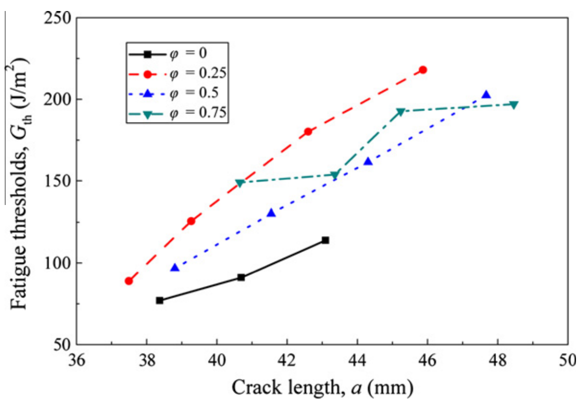

Fig. 9. Fatigue thresholds evaluated by G_{th} versus crack length.

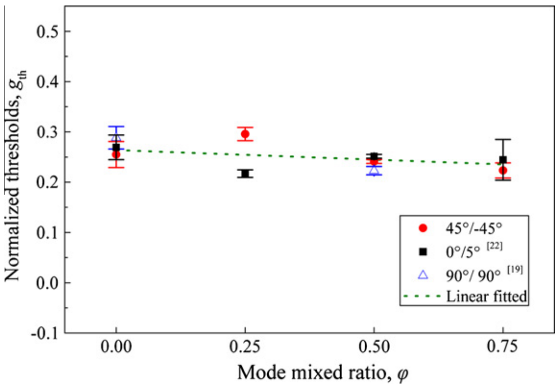

Fig. 10. Average values and standard deviations of the normalized fatigue thresholds.

specimens manufactured by the same materials were also presented in the figure. Despite the difference under the mode mixture ratio of 0.25, it is interesting to observe that all the normalized threshold values are quite close to each other at certain mode mixture ratios. With the mode mixture ratio increasing, average value of the normalized thresholds almost linearly decreased. Thus a uniform formula shown in Eq. (11) was used to fit the experimental data. Fitting result was included in Fig. 10 and good agreement could be concluded.

$$g_{th} = \rho_1 + \rho_2 \varphi \tag{11}$$

As a result, a interface-independent fatigue thresholds was obtained, which could give a simple and efficient guideline to the design of laminates considering delamination growth.

5. Conclusion

The crack growth behavior of 45°/−45° interface laminates under mixed I/II modes was experimentally studied. The *R*-curves obtained from static tests indicated that an increasing delamination resistance, which was found to have significant effect on the fatigue crack growth. The normalized SERR instead of original SERR was therefore utilized as the controlling parameter to evaluate the fatigue crack growth rates and thresholds. The following conclusion could be drawn.

1. The initiation and propagation values of fracture toughness measured under high mode mixture ratio are larger than that under low mixture ratios. All *R*-curves agreed well to the linear fitting within the crack length range from 35 mm to 50 mm, i.e. $1.4 < a/b < 2.0$.
2. The fatigue delamination resistance was found approximately equal to the static fracture toughness for 45°/−45° interface.
3. Due to the *R*-curve effects, the traditional Paris Law plots differed from each other significantly for specimens applied different maximum displacements. Instead, modified Paris Law with the normalized SERR as the controlling parameter gave excellent agreement with test data.
4. An interface-independent fatigue threshold was obtained for 45°/−45°, 0°/5° and 90°/90° laminates, which decrease with increasing mode mixture ratio. This gives a simple guideline for the design of multidirectional composite laminates.

References

[1] Davies P, Blackman BRK, Brunner AJ. Standard test methods for delamination resistance of composite materials: current status. Appl Compos Mater 1998;5(6):345–64.
[2] Brunner AJ, Blackman BRK, Davies P. A status report on delamination resistance testing of polymer–matrix composites. Engng Fract Mech 2008;75(9):2779–94.
[3] Andersons J, Kig M. Dependence of fracture toughness of composite laminates on interface ply orientations and delamination growth direction. Compos Sci Technol 2004;64(13–14):2139–52.
[4] Davidson BD, Bialaszewski RD, Sainath SS. A non-classical, energy release rate based approach for predicting delamination growth in graphite reinforced laminated polymeric composites. Compos Sci Technol 2006;66(10):1479–96.
[5] Quispitupa A, Berggreen C, Carlsson L. On the analysis of a mixed mode bending sandwich specimen for debond fracture characterization. Engng Fract Mech 2009;76(4):594–613.
[6] de Morais A, Pereira A. Mixed mode I + II interlaminar fracture of glass/epoxy multidirectional laminates Part 1: Analysis. Compos Sci Technol 2006;66(13):1889–95.
[7] Naghipour P, Bartsch M, Chernova L, Hausmann J, Voggenreiter H. Effect of fiber angle orientation and stacking sequence on mixed mode fracture toughness of carbon fiber reinforced plastics: numerical and experimental investigations. Mater Sci Eng: A 2010;527(3):509–17.
[8] Sorensen L, Botsis J, Gmr T, Humbert L. Bridging transactions in mode I delamination: measurements and simulations. Compos Sci Technol 2008;68(12):2350–8.

[9] Szekrényes A, Uj J. Advanced beam model for fiber-bridging in unidirectional composite double-cantilever beam specimens. Engng Fract Mech 2005;72(17):2686–702.
[10] Tamuzs V, Tarasovs S, Vilks U. Progressive delamination and fiber bridging modeling in double cantilever beam composite specimens. Engng Fract Mech 2001;68(5):513–25.
[11] Gustafson CG, Hojo M. Delamination fatigue crack growth in unidirectional graphite/epoxy laminates. J Reinf Plast Compos 1987;6(1):36–52.
[12] Hojo M, Nakashima K, Kusaka T, Tanaka M, Adachi T, Fukuoka T, et al. Mode I fatigue delamination of Zanchor-reinforced CF/epoxy laminates. Int J Fatigue 2010;32(1):37–45.
[13] Blanco N, Gamstedt EK, Asp LE, Costa J. Mixed-mode delamination growth in carbon-fibre composite laminates under cyclic loading. Int J Solids Struct 2004;41(15):4219–35.
[14] Asp LE, Sjögren A, Greenhalgh ES. Delamination growth and thresholds in a carbon/epoxy composite under fatigue loading. J Compos Technol Res 2001;23(2):55–68.
[15] Brunner AJ, Murphy N, Pinter G. Development of a standardized procedure for the characterization of interlaminar delamination propagation in advanced composites under fatigue mode I loading conditions. Engng Fract Mech 2009;76(18):2678–89.
[16] Singh S, Greenhalgh E. Mixed-mode delamination growth in carbon-fiber composites under fatigue loading. Tech rep; report DRA/SMC/CR961052/1.0 defence research agency; 1996.
[17] Argüelles A, Viña J, Fernández-Canteli A, Viña I, Bonhomme J. Influence of the matrix constituent on mode I and mode II delamination toughness in fiber-reinforced polymer composites under cyclic fatigue. Mech Mater 2011;43(1):62–7.
[18] Kenane M, Azari Z, Benmedakhene S, Benzeggagh ML. Experimental development of fatigue delamination threshold criterion. Compos Part B: Engng 2011;42(3):367–75.
[19] Peng L, Zhang J, Zhao L, Bao R, Yang H, Fei B. Mode I delamination growth of multidirectional composite laminates under fatigue loading. J Compos Mater 2011;45(10):1077–90.
[20] Argüelles A, Viña J, Canteli AF, Castrillo MA, Bonhomme J. Interlaminar crack initiation and growth rate in a carbon–fibre epoxy composite under mode-I fatigue loading. Compos Sci Technol 2008;68(12):2325–31.
[21] Shivakumar KN, Chen H, Abali F, Le D, Davis C. A total fatigue life model for mode I delaminated composite laminates. Int J Fatigue 2006;28(1):33–42.
[22] Zhang J, Peng L, Zhao L, Fei B. Fatigue delamination growth rates and thresholds of composite laminates under mixed mode loading. Int J Fatigue 2012;40:7–15.
[23] Hiley MJ. Delamination between multi-directional ply interfaces in carbon-epoxy composites under static and fatigue loading. Eur Struct Integr Soc 2000;27:61–72.
[24] Brandt F. A new load introduction concept for improved and simplified delamination beam testing. Exp Tech 1998;22(1):17–20.
[25] Reeder JR, Crews Jr JH. Redesign of the mixed-mode bending delamination test to reduce nonlinear effects. J Compos Technol Res 1992;14(1):12–9.
[26] Reeder Jr JR, Crews JR. Mixed-mode bending method for delamination testing. AIAA J 1990;28(7):1270–6.
[27] Standard test method for mixed mode I–mode II interlaminar fracture toughness of uniderectional fiber reinforced polymer matrix composites. In: ASTM D6671M-06. American Society for Testing and Materials; 2006.
[28] Hashemi S, Kinloch AJ, Williams JG. Mechanics and mechanisms of delamination in a poly(ether sulphone)-fibre composite. Compos Sci Technol 1990;37(4):429–62.
[29] Williams JG. End corrections for orthotropic DCB specimens. Compos Sci Technol 1989;35(4):367–76.
[30] Hashemi S, Kinloch AJ, Williams JG. Corrections needed in double-cantilever beam tests for assessing the interlaminar failure of fibre-composites. J Mater Sci Lett 1989;8(2):125–9.
[31] Wilkins DJ, Eisenmann JR, Camin RA, Margolis WS, Benson RA. Characterizing delamination growth in graphite–epoxy. In: Reifsnider KL, editor. Damage in composite materials, ASTM STP 775. American Society for Testing and Materials; 1982. p. 168–83.
[32] Choi NS, Kinloch AJ, Williams JG. Delamination fracture of multidirectional carbon-fiber/epoxy composites under mode I, mode II and mixed-mode I/II loading. J Compos Mater 1999;33(1):73–100.
[33] Martin RH, Murri GB. Characterization of mode I and mode II delamination growth and thresholds in graphite/peek composites. Tech rep; TM 100577. NASA; 1988.